Circularly/Linearly Polarized and Pattern-Reconfigurable MIMO Millimeter-Wave Antenna

Zhonghe Zhang, *Member, IEEE*, Youquan Wen, Sai-Wai Wong, *Senior Member, IEEE*, Asif Khan, Chaoyun Song, *Senior Member, IEEE*, and Yejun He, *Senior Member, IEEE*

***Abstract*—In this letter, a metal wall reconfigurable millimeter-wave (MMW) polarization/radiation pattern-reconfigurable multiple-input–multiple-output (MIMO) cavity antenna is presented. First, different modes are excited within the same cavity. Then, the metal wall is used to adjust these modes, with a single slot enabling linear polarization and a crossed slot enabling circular polarization, allowing dynamic control of both polarization and radiation direction. Finally, a MIMO antenna prototype operating at a center frequency of 28.2 GHz is fabricated and tested. In both states, good isolation and gain are achieved, making it suitable for millimeter-wave wireless communication systems.**

***Index Terms*—Millimeter wave, multiple-input–multiple-output (MIMO), pattern-reconfigurable, polarization-reconfigurable.**

I. Introduction

The synergistic application of mmWave [1], multiple-input–multiple-output (MIMO) [2], and reconfigurable technologies [3] meets 5G's demand for high-speed, high-capacity data transmission. It also significantly enhances spectral efficiency and communication quality through extended coverage and dynamic antenna tuning, serving as a key driver for the evolution of future networks.

Among these technologies, reconfigurable antennas have been widely investigated, primarily utilizing electronic tuning methods. PIN diodes [4], [5], varactors [6], and microelectromechanical system (MEMS) devices [7] are employed to adjust antenna current and field distribution, achieving polarization [8] or beam reconfiguration [9]. Alternative strategies include liquid crystal [10] and magnetic tuning [11], [12]. At millimeter-wave frequencies, beam reconfiguration can also be achieved using graphene-tuned resistors [13]. This is implemented in an antenna composed of a back-to-back modified Vivaldi structure, where two symmetrical graphene nanoplate pads are integrated into the feedline for dynamic beam control. By varying their resistance, the antenna's radiation pattern transitions from two opposing beams to a single directional beam.

Received 20 March 2025; revised 19 May 2025; accepted 6 June 2025. Date of publication 10 June 2025; date of current version 8 September 2025. This work was supported in part by the National Key Research and Development Program of China under Grant 2023YFE0107900; in part by the National Natural Science Foundation of China under Grant 62071306, Grant 62101341, and Grant 62171289; in part by the Hunan Provincial Natural Science Foundation of China under Grant 2025JJ70174; and in part by the State Key Laboratory of Radio Frequency Heterogeneous Integration under Independent Scientific Research Program 2024012. *(Corresponding author: Sai-Wai Wong.)*

Zhonghe Zhang is with the State Key Laboratory of Radio Frequency Heterogeneous Integration, College of Physics and Optoelectronic Engineering, College of Electronics and Information Engineering, Shenzhen University, Shenzhen 518060, China.

Youquan Wen, Sai-Wai Wong, Chaoyun Song, and Yejun He are with the State Key Laboratory of Radio Frequency Heterogeneous Integration, College of Electronics and Information Engineering, Shenzhen University, Shenzhen 518060, China (e-mail: wongsaiwai@ieee.org).

Asif Khan is with the Department of Electronic and Electrical Engineering, Southern University of Science and Technology, Shenzhen 518055, China.

Digital Object Identifier 10.1109/LAWP.2025.3578485

TABLE I
Comparisons With Reported Millimeter-Wave Reconfigurable Antennas

Ref.	Antenna	Method	Direction	Polarization
[4]	Patch	Pin	0°	RHCP/LHCP/LP
[5]	Patch	Pin	-45°/45°	LP
[13]	Patch	Graphene	0°/180°	LP
[21]	Cavity	Rotation	0°	5 LP
This work	Metal cavity	Metal wall	0°/90°	HP/RHCP

Electronic tuning offers fast switching, while mechanical reconfiguration provides lower cost, low power consumption, and high stability, making it more practical for energy-sensitive devices or high-power applications. Metal screws serve as an effective means of mechanical reconfiguration. In [14], cavity modes are adjusted to alter array antenna polarization and frequency. In [15], an approach is presented to realize eight radiation modes within a rectangular waveguide network. Additionally, simple physical deformation can reshape antenna beams, as demonstrated in [16], where two movable metal strips reconfigure a sectoral horn antenna's half-power beamwidth. Liquid metal [17], [18] serves as a reconfigurable mechanism. In [17], four tunable frequency bands allow transitions between dual circular and linear polarization. In [19], a microfluidic pump redistributes liquid metal to modify surface currents, enabling polarization reconfiguration. This method is convenient for single-element tuning but demands individual reconfiguration modules for each antenna in multi-antenna systems, adding complexity. Mechanical rotation offers another means of tuning antenna properties. In [20], a mechanically reconfigurable patch antenna achieves polarization diversity by rotating between left-hand and right-hand circular polarization. Such methods are applicable in the millimeter-wave band [21], where a multilinear polarization-reconfigurable antenna utilizes a TM_{510} resonant air-filled cavity as the substrate, forming an array with five linear polarization states.

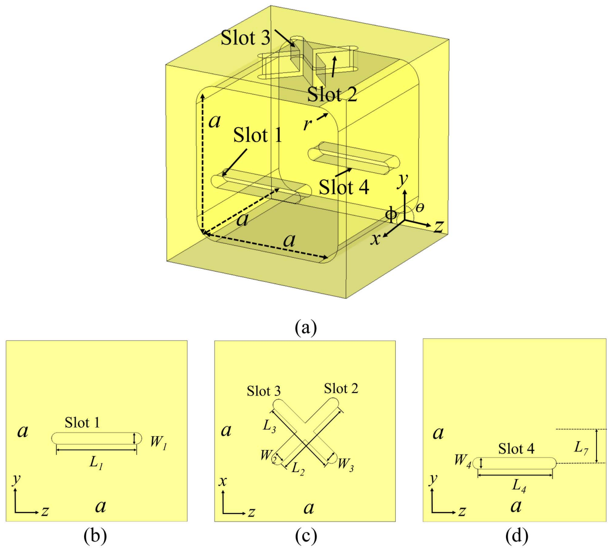

Fig. 1. Configuration of the proposed antenna. (a) 3-D view. (b) Front view. (c) Top view. (d) Back view. Dimensions (unit: mm): $a = 7.4$, $L_1 = 4.08$, $W_1 = 0.6$, $L_2 = 3.88$, $W_2 = 0.6$, $L_3 = 4.09$. $W_3 = 0.6$, $L_4 = 3.7$, $W_4 = 0.6$.

As shown in Table I, which compares reported millimeter-wave reconfigurable antennas, current mechanical reconfiguration technologies remain limited at these frequencies. However, the demand for antenna polarization and beam reconfigurability is increasing, particularly for designs that enable simultaneous control of beam direction and polarization. This letter presents a metal wall-based reconfigurable method for millimeter-wave applications. The design is based on a cavity structure and combines reconfigurable antennas with MIMO technology, achieving linear/circular polarization reconfigurability in a four-element antenna and enabling 90° beam steering.

II. Antenna Design and Analysis

A. Antenna Structure

The configuration of the proposed antenna is shown in Fig. 1. Fig. 1(a) presents a 3-D view of the antenna, which consists of a metal cavity with slots on three of its faces. Fig. 1(b) shows the front view of the antenna, with Slot 1 as the radiation slot. Fig. 1(c) shows the top view of the antenna, where Slots 2 and 3 are also radiation slots. Fig. 1(d) shows the rear view of the antenna, with Slot 4 as the feeding slot. It is worth noting that the antenna cannot operate in this state, and the antenna impedance is mismatched. The specific operating conditions are provided below.

Unlike traditional mechanical reconfiguration methods, this letter proposes a novel method of reconfiguration using metal walls. In the front or top view of Fig. 1, metal walls are used to block certain slots, allowing the unblocked radiation slots to operate. The metal wall functions like a switch, adjusting the states of the antenna to achieve radiation in different directions and polarizations. To evaluate the effectiveness of the proposed design, all electromagnetic simulations including *S*-parameters and far-field radiation characteristics were performed using CST Microwave Studio.

B. Reconfigurable HP Antenna Design

The configuration of the proposed horizontally polarized (HP) antenna is shown in Fig. 2. Unlike Fig. 1(a), the top of the metal cavity has a layer of metal wall, which blocks Slot 2 and Slot 3. In this case, Slot 2 and Slot 3 do not operate. Slot 4 serves as the feeding slot, exciting the TE_{101} mode inside the cavity. The resonant frequency of the mode is determined by (1). The magnetic permeability and permittivity of vacuum are represented by μ_r and ε_r. The speed of light is indicated by υ, and a specifies the internal dimension of the cavity [22].

$$f_{101} = \frac{\sqrt{2}\upsilon}{2a\sqrt{\mu_r \varepsilon_r}}. \quad (1)$$

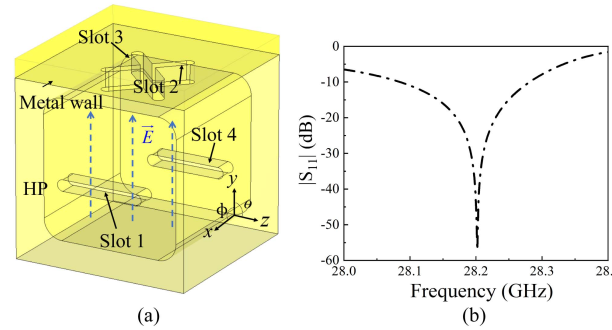

Fig. 2. (a) Configuration of the proposed HP antenna. (b) $|S_{11}|$.

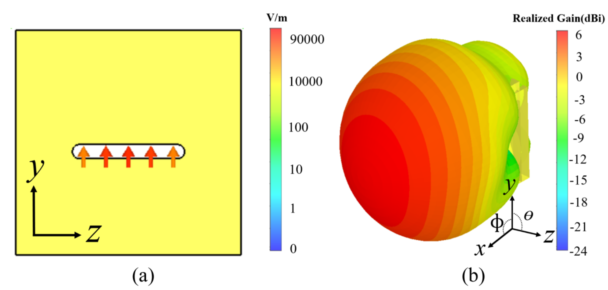

Fig. 3. (a) Electric field distribution of the antenna slots at 28.2 GHz. (b) Radiation pattern at 28.2 GHz.

The blue arrows in the figure indicate the direction of the electric field inside the cavity, which is parallel to the y-axis and perpendicular to the *x*-axis. Fig. 2(b) shows the simulated antenna return loss, with the antenna resonating at 28.2 GHz.

Fig. 3(a) shows the electric field distribution of the antenna slots at 28.2 GHz. The center of the cavity is where the field strength is the strongest. A slot is opened at the center to achieve HP beam radiation. Fig. 3(b) shows the radiation pattern at 28.2 GHz, with the antenna achieving beam coverage directed towards the $+x$-direction.

C. Reconfigurable RHCP Antenna Design

As illustrated in Fig. 5, the configuration of the proposed RHCP antenna differs from Fig. 3(a) in that a metal wall is placed in front of the antenna, blocking Slot 1. Consequently, slot 1 is inactive. Feeding slot 4 excites the TE_{011} mode within the cavity, and the resonant frequency of this mode is determined by the following equation [22]:

$$f_{011} = \frac{\sqrt{2}\upsilon}{2a\sqrt{\mu_r \varepsilon_r}}. \quad (2)$$

It can be observed that the resonances of the two modes occur at the same frequency. This is because the cavity is a square metal cavity, which also forms the basis for tuning the two

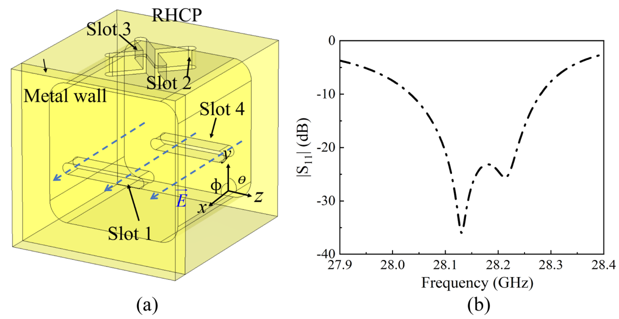

Fig. 4. (a) Configuration of the proposed RHCP antenna. (b) $|S_{11}|$.

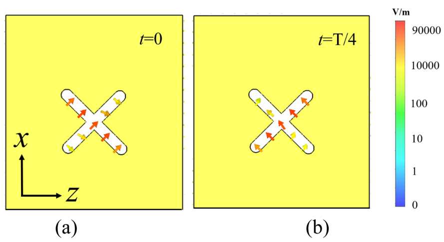

Fig. 5. Electric field distribution of the antenna slots at 28.2 GHz. (a) $t = 0$. (b) $t =$ T/4.

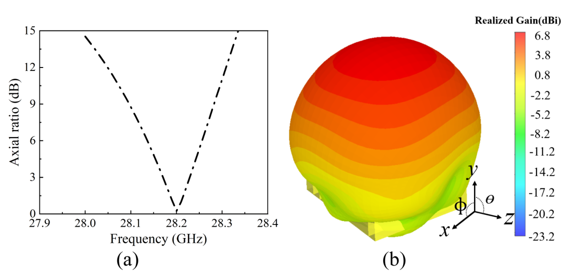

Fig. 6. (a) AR. (b) Radiation pattern at 28.2 GHz.

states. The blue arrows in Fig. 4(a) indicate the direction of the electric field inside the cavity, which is perpendicular to the y-axis and parallel to the x-axis. Slots 2 and 3 are in operation, positioned at a 90° angle to each other. Both slots intersect the electric field direction at a 45° angle. This design is intended to achieve circular polarization. Fig. 4(b) shows the return loss of the antenna. It can be observed that the antenna has two resonance points, each corresponding to the lengths of Slots 2 and 3.

The electric field distribution of the antenna slots at 28.2 GHz is shown in Fig. 5. At $t = 0$, the electric field direction is perpendicular to the long edge of Slot 3. At $t =$ T/4, the electric field direction is perpendicular to the long edge of Slot 2. The electric field directions are perpendicular to each other and have a phase difference of 90°, thereby achieving circular polarization. Fig. 6(a) shows the axial ratio of the circularly polarized antenna, which remains below 3 dB at 28.2 GHz. Fig. 6(b) illustrates the radiation pattern at the same frequency, demonstrating circularly polarized beam coverage in the $+y$-direction.

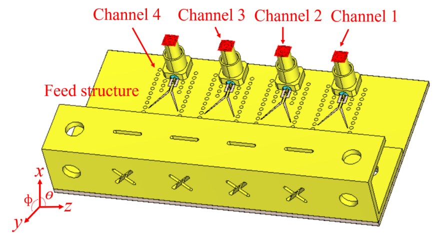

Fig. 7. Configuration of the proposed reconfigurable antenna.

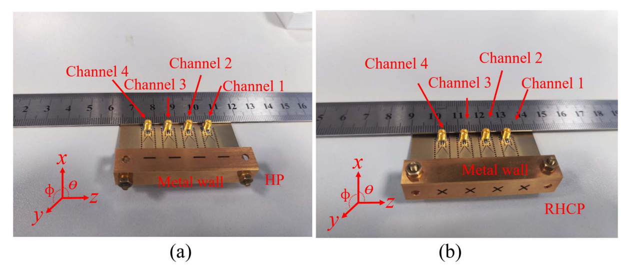

Fig. 8. Fabricated prototype of the reconfigurable antenna. (a) State 1 (b) State 2.

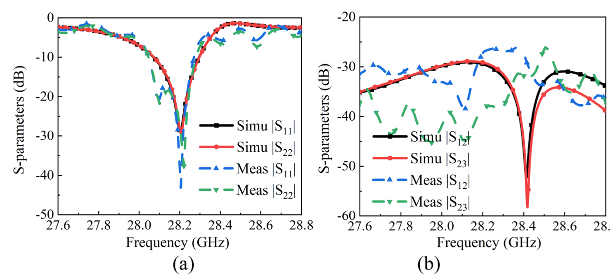

Fig. 9. Simulated and measured S-parameters. (a) Return loss. (b) Isolation.

III. MIMO Design and Measurement

A 1 × 4 MIMO antenna is designed to support diverse directions and diverse polarization millimeter-wave signal transmission. The configuration of the proposed reconfigurable antenna is shown in Fig. 7. The antenna adopts a full-metal cavity structure, with the printed circuit board (PCB) feed ports located at the bottom. However, the antenna structure in its initial state cannot operate due to impedance mismatch. The reconfigurable MIMO antenna features two distinct states, and adjustments between these states are achieved by controlling metal wall.

A. MIMO Reconfigurable HP Antenna

The fabricated prototype of the reconfigurable antenna is shown in Fig. 8, where Fig. 8(a) represents State 1, consisting of four cavity antennas. The antenna achieves HP polarization directed toward the x-axis. The simulated and measured S-parameters are presented in Fig. 9, with the return loss shown in Fig. 9(a) and the isolation of symmetric ports in Fig. 9(b). The port return loss is better than 10 dB, and the isolation between adjacent ports exceeds 25 dB. Reasonable consistency is observed, satisfying the requirements for both radiation and isolation.

Fig. 10 shows the simulated and measured results of the MIMO reconfigurable HP antenna. The xoy-plane is the E-plane, and the xoz-plane is the H-plane. Both radiation patterns align well, with a beam-pointing angle of phi = 0°. Compared to

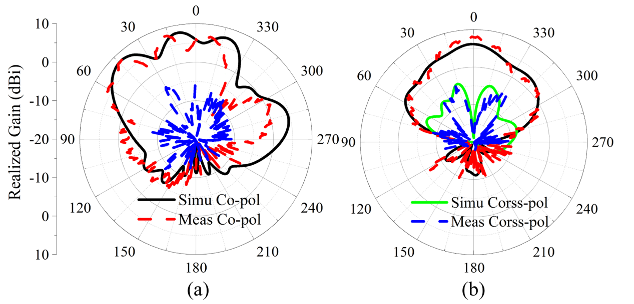

Fig. 10. Simulated and measured results of the MIMO reconfigurable HP antenna. (a) *xoy*-plane (b) *xoz*-plane.

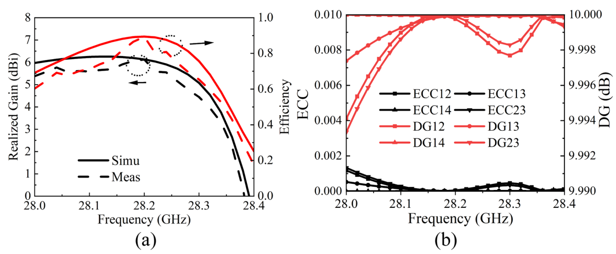

Fig. 11. Simulated and measured realized gain and ECC of the MIMO reconfigurable HP antenna. (a) Realized gain and efficiency. (b) ECC and DG.

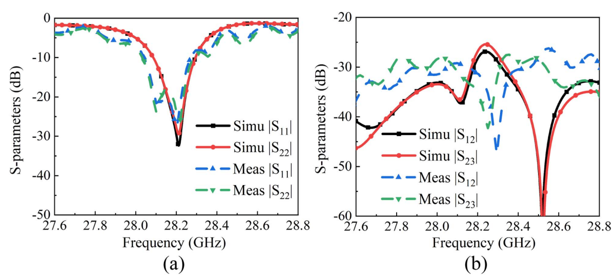

Fig. 12. Simulated and measured *S*-parameters. (a) Return loss. (b) Isolation.

Fig. 3(b), sidelobes are generated in the antenna's E-plane due to the feed structure, which can be avoided in practical applications.

Fig. 11 shows the simulated and measured realized gain, efficiency, and envelope correlation coefficient (ECC) of the MIMO reconfigurable HP antenna. Fig. 11(a) presents the realized gain and antenna efficiency, with a tested gain of 6.13 dBi and a measured efficiency of 89.3%. When the reconfigurable antenna is in State 1, the diversity performance of the MIMO antenna at 28.2 GHz is evaluated through far-field testing and algorithmic calculation using the ECC and diversity gain (DG), as shown in Fig. 11(b). The measured ECC is less than 0.001, and the DG exceeds 9.99 dB, demonstrating the excellent diversity performance of the MIMO antenna.

B. MIMO Reconfigurable RHCP Antenna

The fabricated prototype of the MIMO reconfigurable RHCP antenna is shown in Fig. 8(b). In this configuration, a metal wall is placed on top of the antenna, blocking the radiation slots in the *x*-direction. Meanwhile, the cross slots in the *y*-direction are exposed, generating right-hand circularly polarized radiation. Fig. 12(a) presents the return loss, while Fig. 12(b) shows the isolation between symmetric ports. Both simulated and measured isolation values remain below 25 dB, indicating good consistency and meeting the radiation and isolation requirements.

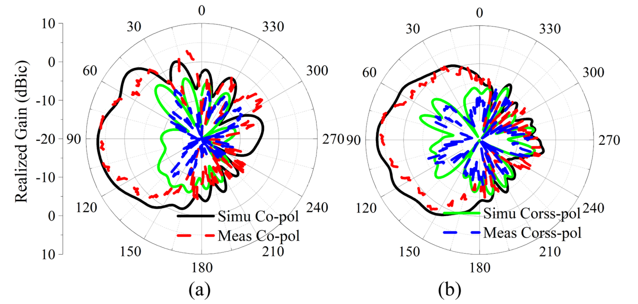

Fig. 13. Simulated and measured results of the MIMO reconfigurable RHCP antenna. (a) *xoy*-plane (b) *yoz*-plane.

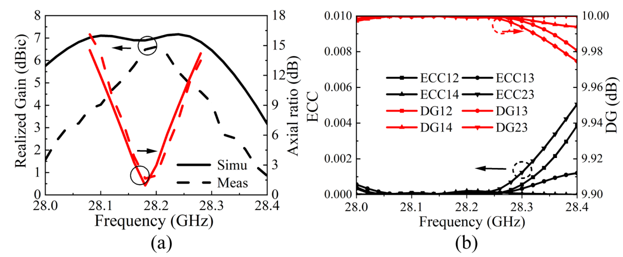

Fig. 14. Simulated and measured realized gain and ECC of the MIMO reconfigurable RHCP antenna. (a) Realized gain and AR. (b) ECC and DG.

Fig. 13 shows the simulated and measured results of the MIMO reconfigurable RHCP antenna. The radiation patterns are consistent, with a beam-pointing angle of phi = 90°. The simulated and measured realized gain and AR of the MIMO reconfigurable RHCP antenna are shown in Fig. 14(a). At 28.2 GHz, the measured gain is 6.61 dBic, and the simulated gain is 6.99 dBic, showing good agreement at the resonant frequency. The rapid gain drop outside the resonance is attributed to CNC fabrication tolerances. Both the simulated and measured AR values are below 3 dB at 28.2 GHz, indicating excellent circular polarization performance. In State 2, the reconfigurable RHCP antenna's diversity performance at 28.2 GHz is evaluated through far-field testing and algorithmic analysis, as shown in Fig. 14(b). Additionally, the measured efficiency of the antenna at 28.2 GHz reached 79%. The results indicate that the ECC is less than 0.001, and the DG exceeds 9.99 dB, demonstrating the excellent diversity performance of the MIMO antenna. The new mechanical reconfiguration approach introduces novel antenna characteristics. The full metal antenna achieves high power handling capability while enabling circular/linear polarization switching and 90° beam direction switching within the millimeter-wave band.

IV. Conclusion

In this letter, we design a polarization-and radiation pattern-reconfigurable antenna using a cavity structure and metal walls. The antenna's polarization can switch between linear and circular polarization, and its radiation pattern can switch between two mutually perpendicular directions. The antenna operates in the millimeter-wave frequency band and supports a MIMO mode. The design of the metal walls provides a new approach for millimeter-wave mechanically reconfigurable antennas, with potential applications in the field of MIMO wireless communication.

REFERENCES

[1] J. Huang, C.-X. Wang, H. Chang, J. Sun, and X. Gao, "Multi-frequency multi-scenario millimeter wave MIMO channel measurements and modeling for B5G wireless communication systems," *IEEE J. Sel. Areas Commun.*, vol. 38, no. 9, pp. 2010–2025, Sep. 2020.

[2] A. Alkhateeb, J. Mo, N. Gonzalez-Prelcic, and R. W. Heath, "MIMO precoding and combining solutions for millimeter-wave systems," *IEEE Commun. Mag.*, vol. 52, no. 12, pp. 122–131, Dec. 2014.

[3] S.-L. Chen, F. Wei, P.-Y. Qin, Y. J. Guo, and X. Chen, "A multi-linear polarization reconfigurable unidirectional patch antenna," *IEEE Trans. Antennas Propag.*, vol. 65, no. 8, pp. 4299–4304, Aug. 2017.

[4] M. P. Singh, T. Tomura, J. Hirokawa, and S. Ghosh, "A compact wideband millimeter-wave polarization-reconfigurable antenna array," *IEEE Antennas Wireless Propag. Lett.*, vol. 24, no. 3, pp. 691–695, Mar. 2025.

[5] K. Trzebiatowski, M. Rzymowski, L. Kulas, and K. Nyka, "Simple 60 GHz switched beam antenna for 5G millimeter-wave applications," *IEEE Antennas Wireless Propag. Lett.*, vol. 20, no. 1, pp. 38–42, Jan. 2021.

[6] S. Xiao, C. Zheng, M. Li, J. Xiong, and B.-Z. Wang, "Varactor-loaded pattern reconfigurable array for wide-angle scanning with low gain fluctuation," *IEEE Trans. Antennas Propag.*, vol. 63, no. 5, pp. 2364–2369, May 2015.

[7] T. J. Jung, I.-J. Hyeon, C.-W. Baek, and S. Lim, "Circular/linear polarization reconfigurable antenna on simplified RF-MEMS packaging platform in K-band," *IEEE Trans. Antennas Propag.*, vol. 60, no. 11, pp. 5039–5045, Nov. 2012.

[8] J. M. Kovitz, H. Rajagopalan, and Y. Rahmat-Samii, "Design and implementation of broadband MEMS RHCP/LHCP reconfigurable arrays using rotated E-shaped patch elements," *IEEE Trans. Antennas Propag.*, vol. 63, no. 6, pp. 2497–2507, Jun. 2015.

[9] G. H. Huff and J. T. Bernhard, "Integration of packaged RF MEMS switches with radiation pattern reconfigurable square spiral microstrip antennas," *IEEE Trans. Antennas Propag.*, vol. 54, no. 2, pp. 464–469, Feb. 2006.

[10] J. Yang et al., "Fully electronically phase modulation of millimeter-wave via comb electrodes and liquid crystal," *IEEE Antennas Wireless Propag. Lett.*, vol. 20, no. 3, pp. 342–345, Mar. 2021.

[11] S. Zhao, Z. Wang, and Y. Dong, "Pattern-reconfigurable antenna using low-profile electric and magnetic radiators," *IEEE Antennas Wireless Propag. Lett.*, vol. 22, no. 3, pp. 616–620, Mar. 2023.

[12] U. Myrzakhan, F. A. Ghaffar, M. Vaseem, and A. Shamim, "Additively-manufactured, magnetically controlled, frequency and polarization reconfigurable phased array antenna," *IEEE Open J. Antennas Propag.*, vol. 6, no. 1, pp. 264–273, Feb. 2025.

[13] C. Fan, B. Wu, Y. Hu, Y. Zhao, and T. Su, "Millimeter-wave pattern reconfigurable vivaldi antenna using tunable resistor based on graphene," *IEEE Trans. Antennas Propag.*, vol. 68, no. 6, pp. 4939–4943, Jun. 2020.

[14] R.-S. Chen et al., "Reconfigurable full-metal circularly-polarized cavity-backed slot antenna and array with frequency and polarization agility," *IEEE Trans. Circuits Syst. II, Exp. Briefs*, vol. 70, no. 2, pp. 531–535, Feb. 2023.

[15] P. Sanchez-Olivares and J. L. Masa-Campos, "Mechanically reconfigurable conformal array antenna fed by radial waveguide divider with tuning screws," *IEEE Trans. Antennas Propag.*, vol. 65, no. 9, pp. 4886–4890, Sep. 2017.

[16] A. Jouade, M. Himdi, A. Chauloux, and F. Colombel, "Mechanically pattern-reconfigurable bended horn antenna for high-power applications," *IEEE Antennas Wireless Propag. Lett.*, vol. 16, pp. 457–460, 2017.

[17] L. Li, X. Yan, H. C. Zhang, and Q. Wang, "Polarization- and frequency-reconfigurable patch antenna using gravity-controlled liquid metal," *IEEE Trans. Circuits Syst. II, Exp. Briefs*, vol. 69, no. 3, pp. 1029–1033, Mar. 2022.

[18] V. T. Bharambe, J. Ma, M. D. Dickey, and J. J. Adams, "RESHAPE: A liquid metal-based reshapable aperture for compound frequency, pattern, and polarization reconfiguration," *IEEE Trans. Antennas Propag.*, vol. 69, no. 5, pp. 2581–2594, May 2021.

[19] H. Xing et al., "Three-polarization-reconfigurable antenna array implemented by liquid metal," *IEEE Antennas Wireless Propag. Lett.*, vol. 23, no. 1, pp. 374–378, Jan. 2024.

[20] I. T. McMichael, "A mechanically reconfigurable patch antenna with polarization diversity," *IEEE Antennas Wireless Propag. Lett.*, vol. 17, no. 7, pp. 1186–1189, Jul. 2018.

[21] S.-L. Chen, Y. Liu, H. Zhu, D. Chen, and Y. J. Guo, "Millimeter-wave cavity-backed multi-linear polarization reconfigurable antenna," *IEEE Trans. Antennas Propag.*, vol. 70, no. 4, pp. 2531–2542, Apr. 2022.

[22] J.-Y. Lin, Y. Yang, S.-W. Wong, X. Li, L. Wang, and E. Dutkiewicz, "Two-way waveguide diplexer and its application to diplexing In-band full-duplex antenna," *IEEE Trans. Microw. Theory Techn.*, vol. 71, no. 3, pp. 1171–1179, Mar. 2023.